Available online at www.sciencedirect.com

SciVerse ScienceDirect

Ceramics International 39 (2013) 4179–4186

CERAMICS INTERNATIONAL

www.elsevier.com/locate/ceramint

Structural and magnetic properties of the copper ferrite obtained by reactive milling and heat treatment

Traian Florin Marinca[a,*], Ionel Chicinaş[a], Olivier Isnard[b]

[a]*Materials Science and Engineering Department, Technical University of Cluj-Napoca, 103-105 Muncii Avenue, 400641 Cluj-Napoca, Romania*
[b]*Institut Néel, CNRS/Université Joseph Fourier, BP166, 38042 Grenoble, Cédex 9, France*

Received 29 August 2012; received in revised form 30 October 2012; accepted 31 October 2012
Available online 10 November 2012

Abstract

Copper ferrite ($CuFe_2O_4$) was synthesised from an equimolar mixture of copper and iron oxides by mechanosynthesis and subsequent heat treatment. After mechanosynthesis, depending on the milling time, the powder consists in a mixture of phases. The heat treatment at 600 °C did not lead to a complete reaction of the mechano-activated precursors. After the heat treatments at 800 and 1000 °C, the complete formation of copper ferrite for almost all the milling times was noticed. The crystal structure of the copper ferrite was found to be cubic for all the samples heat treated at 1000 °C and a mixture of tetragonal and cubic for the samples heat treated at 800 °C. The amount of copper ferrite with cubic structure predominates in the samples with prolonged milling duration and a decrease of the tetragonal distortion by increasing the milling time occurs. The crystallisation of $CuFe_2O_4$ in cubic structure for the samples milled for prolonged time is influenced by the powder contamination with iron. The magnetisations of the samples obtained after heat treatment at 1000 °C were found to be larger compared to the ones of the samples heat treated at 800 °C. The iron contamination, milling duration and heat treatment temperature influence the cations distribution, thus leading to the saturation magnetisation of the copper ferrite samples ranging from 11.9 μ_B/f.u. to 16.4 μ_B/f.u.

Keywords: A. Milling; B. X-ray methods; C. Magnetic properties; D. Ferrites

1. Introduction

Spinel soft ferrites ($MeFe_2O_4$, where Me is metal or a group of metallic elements with 2^+ as total valence) represent one of the most important group of magnetic materials, due to their interesting characteristics. This class of magnetic materials is very important, from both fundamental research and technical applications [1–5]. Their remarkable features are given by their spinel structure. Soft magnetic ferrites are isostructural with the mineral spinel $MgAl_2O_4$. Their complex characteristic crystal structure is a face-centered cubic (space group Fd3m) which has eight formula units in unit cell. For the metallic cations are two crystallographic sites: tetrahedral (A site) and octahedral (B site). The distribution of the metallic cations, Me^{2+} and Fe^{3+}, in tetrahedral and octahedral sites (A and B sublattices) has a great importance on the electric and magnetic properties. Typically, there are two types of spinels structures: normal and inverse. In normal spinel, the Me^{2+} cations are positioned in A sites and the Fe^{3+} cations in B sites. In inverse spinel, the Me^{2+} cations are in B sites and the Fe^{3+} cations in both A and B sites. This cations distribution is generally obtained if ferrites are synthesised by classical ceramic route [2,6–9]. Using particular methods such as: sol–gel, mechanosynthesis or co-precipitation, various cations distributions are obtained [10–15]. One of the most interesting soft ferrite is copper ferrite, $CuFe_2O_4$. Copper ferrite has inverse spinel structure, with Cu^{2+} cations in octahedral sites if it is classically obtained from oxides by ceramic techniques [2]. A particular feature of $CuFe_2O_4$ is the possibility of this compound to crystallise in tetragonal spinel with space group $I4_1/amd$. The tetragonal crystal type can be considered as a tetragonally distorted spinel structure with non-standard face-centered space group $F4_1/ddm$ [16]. The origin of this distortion is a cooperative Jahn–Teller effect which is provoked by the alignment of the Cu^{2+} cations

*Corresponding author.
E-mail address: traian.marinca@stm.utcluj.ro (T.F. Marinca).

0272-8842/$ - see front matter © 2012 Elsevier Ltd and Techna Group S.r.l. All rights reserved.
http://dx.doi.org/10.1016/j.ceramint.2012.10.274

positioned in B sublattice formed by the oxygen anions which is tetragonally distorted octahedral sublattice [17]. Using common techniques of ceramics, the cubic structure is obtained if the samples are quenched from above 760 °C and the tetragonal structure is obtained if the samples are slowly cooled [2]. The copper ferrite is ferrimagnetic in both crystal systems due to the antiparallel alignment of the magnetic moments of A and B sublattices. The saturation magnetisation of $CuFe_2O_4$ is about 1 μ_B/molecule if it is classically obtained and could be increased up to 2.3 μ_B/molecule if it is synthesised by other techniques [1]. This increase is given by the positioning of the Cu^{2+} and Fe^{3+} cations in both A and B crystallographic sites, $[Cu^{2+}_{1-x}Fe^{3+}_{x}]^{A}[Fe^{3+}_{2-x}Cu^{2+}_{x}]^{B}O_4$, leading to a larger difference between B and A sublattice magnetisations [9]. Several results regarding the obtaining of the tetragonal or cubic $CuFe_2O_4$ by synthesis routes that involve mechanosynthesis were reported [18–22]. For the synthesis of $CuFe_2O_4$ by these routes various chemical compounds such as carbonates, oxalates, hydroxides, nitrides or oxides were used as precursors [21–23]. The producing of copper ferrite only by mechanosynthesis from stoichiometric mixture of CuO and α-Fe_2O_3 was proved to be very difficult to achieve due to the reversible synthesis–decomposition in Fe–Cu–O system [22,24,25]. Therefore, the mechanosynthesis method is combined with other methods for obtaining $CuFe_2O_4$. The copper ferrite was subjected to mechanosynthesis and a change of the structure from tetragonal to cubic was noticed. The polymorphic transformation is assigned to the destroying of the cooperative Jahn–Teller ordering by the lattice imperfection (dislocation and stacking fault) and to the redistribution of the cations induced by the ball milling process [25,26]. After synthesis by various routes, the subsequent heat treatment is also very important in order to preserve or change the obtained crystal structure of $CuFe_2O_4$ [16,19].

In the present paper, the synthesis of copper ferrite using mechanosynthesis and subsequent heat treatment in both tetragonal and cubic structures is presented.

2. Experimental details

An equimolar mixture of high purity commercial oxide powders (Alpha Aesar), copper oxide (CuO—tenorite) and iron oxide (α-Fe_2O_3—haematite) was subjected to reactive milling (RM) in a planetary ball-mill (Fritsch, Pulverisette 4) up to 30 h. The milling experiments were carried out in similar conditions (ball to powder ratio, BPR = 15:1, vial rotational speed, ω = 800 rpm, disc rotational speed, Ω = −400 rpm) as described in [13,27]. After the milling experiments, the samples were annealed for 6 h in air at different temperatures (600–1000 °C temperature range).

The structural evolution of copper ferrite during milling and after annealing was investigated by X-ray diffraction (XRD) in the angular range 2θ = 20–90°. A Siemens D5000 diffractometer which operates in reflection with CoK_α radiation (λ = 1.7903 Å) was used. The lattice parameter was determined by a least square refinement procedure, taking into account all the observed peak position, (Celref software) [28].

The M(H) curves were recorded at 300 K using the extraction sample method in a continuous magnetic field of up to 8 T [29]. The saturation magnetisation values were derived from the magnetisation curves obtained in the magnetic field higher than 4 T.

3. Results and discussion

Fig. 1 shows the X-ray diffraction patterns recorded for the starting sample (ss), as-milled samples for 4, 8, 12, 16, 20, 24 and 30 h and milled and subsequently annealed for 6 h at 600 °C in air atmosphere samples. In the figures, for each sample the milling time is marked and for the milled and subsequently annealed samples the time and temperature of heat treatment (TT) are marked. The starting sample consists of an equimolar mixture of CuO and α-Fe_2O_3 and, as expected, the diffraction pattern exhibits the corresponding Bragg reflections of these two oxides. In the diffraction patterns recorded for the as-milled samples are noticed Bragg reflections corresponding to various phases, depending on the milling time as we showed in our previous work [22,27]. After 4 h of milling, the material consists of a mixture of CuO–α-Fe_2O_3 solid solution with haematite structure and $CuFe_2O_4$ with cubic spinel structure (c-$CuFe_2O_4$). After 8 h of milling, in material, beside the solid solution and copper ferrite, the cuprite (Cu_2O) phase is also present. The same phases as for the 8 h milled sample are identified in the diffraction patterns of 12 and 16 h milled samples. Increasing the milling duration leads to the formation of new phases. The Bragg reflections corresponding to the elemental Fe are noticed for the samples milled 20, 24 and 30 h, as a result of the powder contamination during milling, in excellent agreement

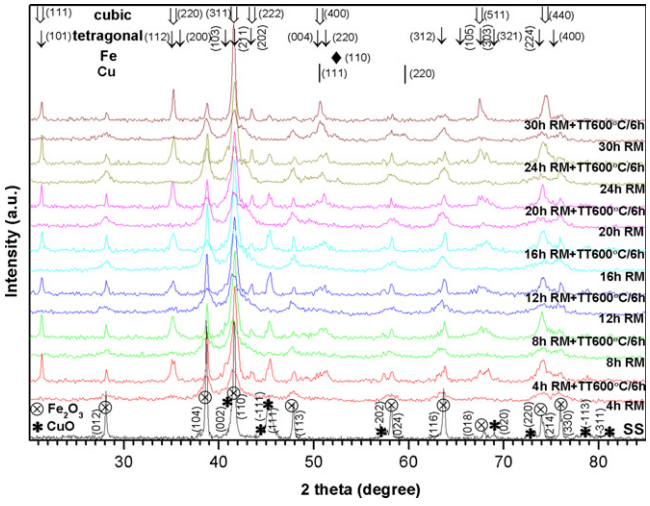

Fig. 1. XRD patterns recorded for the starting sample (ss), as-milled samples (4, 8, 12, 16, 20, 24 and 30 h of milling) and milled and subsequently annealed samples at 600 °C for 6 h in air.

with earlier reported results [13,22,30]. In the diffraction patterns of the 24 and 30 h milled samples, diffraction lines corresponding to the elemental Cu are identified, as a result of the dissociation from the existing copper oxides. This behaviour is discussed in detail in Ref. [22]. A heat treatment at 600 °C for 6 h changes significantly the phase's composition of all the milled samples. For each milling time, the material consists of a mixture of α-Fe_2O_3, CuO and $CuFe_2O_4$. The $CuFe_2O_4$ obtained after 30 h of milling and subsequently heat treated (600 °C/6 h) is crystallised in cubic structure. For the other samples, milled for a shorter duration and heat treated at the same temperature, the copper ferrite is crystallised in both cubic and tetragonal structures. The formation of CuO during this heat treatment is assigned to multiple causes, depending on the different composition of the material at various milling time: the dissolution of Fe_2O_3–CuO solid solution, crystallisation of amorphous CuO, oxidation of Cu_2O and elemental Cu oxidation for prolonged milling times (24 and 30 h). In the samples heat treated at 500 °C for 4 h and at 600 °C for 2 h, the presence of the tetragonal structure of $CuFe_2O_4$ (t-$CuFe_2O_4$) was not remarked [27]. The heat treatment at 600 °C/6 h, on one hand, seems to increase the amount of the c-$CuFe_2O_4$ and, on the other hand, is favourable to the formation of the t-$CuFe_2O_4$. The energy induced in the samples by the ball milling process and by annealing at (600 °C for 6 h) is not sufficient to induce a complete reaction between the phases in order to obtain copper ferrite and therefore, the samples were subjected to heat treatment at 800 and 1000 °C for 6 h in air atmosphere. The XRD patterns recorded for these samples are presented in Fig. 2a. A detail regarding the 2 theta zone, corresponding to the haematite most intense peak, is presented in Fig. 2b. The samples milled up to 20 h and subsequently annealed at 800 °C for 6 h show a complete reaction between the starting oxides. For the samples milled for 24 and 30 h the Bragg reflections of the α-Fe_2O_3 are still noticed and are associated with the small amount of the α-Fe_2O_3 which remains un-reacted. It can be assumed that the α-Fe_2O_3, that is present in these samples after heat treatment, is, in part, due to the excess of Fe provided by the contamination during milling. The amount of the elemental Fe provided by the powder contamination oxidises during heating in air, but the energy transferred to the material during this heat treatment is not enough for a complete reaction in order to form a spinel structure. Using area ratio of the most intense peak of the c-$CuFe_2O_4$ and the one of α-Fe_2O_3 ((311) and (104) respectively), the amount of the un-reacted α-Fe_2O_3 was estimated at 3–4 wt% for the sample milled for 24 h and at 7–8 wt% for the sample milled for 30 h. In all the milled and subsequently annealed samples, at 800 °C for 6 h, the obtained copper ferrite presents both cubic and tetragonal structures, except the sample milled for 30 h which is completely crystallised in cubic structure. The heat treatment at 1000 °C for 6 h leads to a complete reaction of the material constituent phases, resulting in a cubic copper ferrite for all the milling times.

Fig. 3a presents the details of the XRD patterns recorded for the samples milled for 4, 8, 12, 16, 20, 24 and 30 h and subsequently annealed in air at 800 °C and 1000 °C for 6 h, in the 2θ interval where are the most intense Bragg reflections of the t-$CuFe_2O_4$ and c-$CuFe_2O_4$, (211) and (311) respectively. Also, Fig. 3b presents the evolution of the area ratio of these most intense reflections versus milling time for the samples heat treated at 800 °C for 6 h. Beside the heat treatment temperature, the milling time seems to play an important role on the crystal type structure for copper ferrite since, for the same heat treatment temperature but different milling time, the samples consist in different structures. If the 4 h milled sample contains a larger amount of $CuFe_2O_4$ with tetragonal structure, in the 30 h milled sample $CuFe_2O_4$ exhibits only cubic structure. The milling time is very important for the samples heat treated at 800 °C and seems to have no influence for the samples heat treated at 1000 °C since for all the milling times we obtained c-$CuFe_2O_4$ (Fig. 3a). The prolonged milling time leads to the

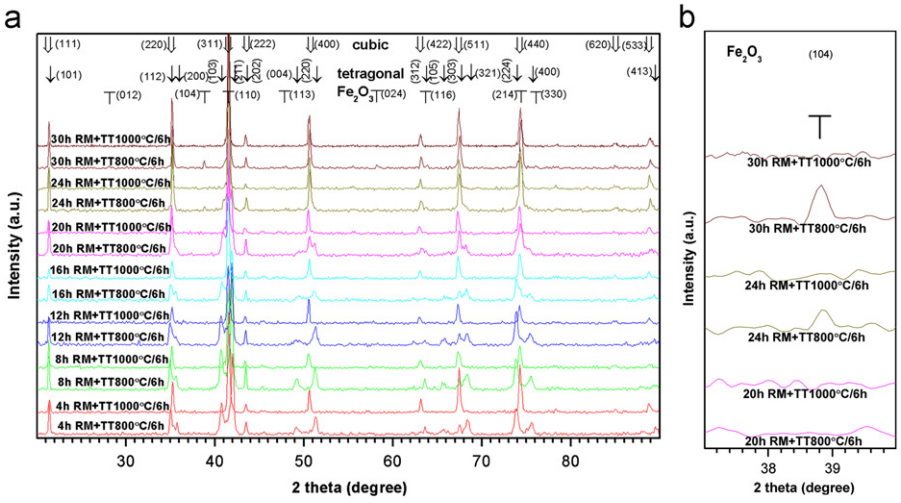

Fig. 2. (a) XRD patterns recorded for the milled and subsequently annealed samples at 800 °C and 1000 °C for 6 h in air and (b) detail of 2 theta zone corresponding to the haematite most intense peak, (104).

increase of the c-$CuFe_2O_4$ amount for the samples heat treated at 800 °C as can be seen in the Fig. 3b, since the area ratio of the tetragonal (211) and cubic (311) reflections decreases down to zero for the 30 h milled sample.

In order to have a quick summary about the various phases which are formed by RM and subsequent heat treatments in air for 6 h at 600, 800 and 1000 °C in Table 1 are given the phases composition of the samples according to the XRD investigations. It is noticeable that both parameters, heat treatment temperature and milling time, have an important role in the formation of different phases in material. Also, the iron contamination seems to play an important role for the samples milled more than 20 h (the presence of the elemental Fe was detected by XRD) while in these samples the presence of the α-Fe_2O_3 after heat treatment at 800 °C is noticed. The supplementary Fe provided by the contamination changes the stoichiometry and leads to the formation of an unwanted phase [31]. After the heat treatment at 1000 °C only copper ferrite with cubic structure was detected by XRD, thus indicating the complete reaction of the elemental Fe provided by the contamination. The obtained copper ferrite has small deviations from the starting stoichiometry, where the Cu:Fe ratio was 1:2 in order to form $CuFe_2O_4$. The copper ferrite is practically a mixed copper–iron ferrite, where the ratio Cu:Fe is 1:(2+γ) and the chemical formula can be written as $Cu_{1-\gamma}Fe_{2+\gamma}O_4$ [22]. By γ was noted the excess of the iron provided by the powder contamination. Even if the elemental iron was detected only for the samples milled 20, 24 and 30 h it can be expected that the contamination started earlier, but it was not detected by XRD due to the small amount of the elemental iron existing in the samples. The amount of the iron resulting from the ball milling contamination increases by increasing the milling time and adjusts the samples stoichiometry [13].

In order to further investigate the influence of the milling time, heat treatment temperature and contamination with iron on copper ferrite structure, the lattice parameters for both tetragonal and cubic structures were calculated, for each sample. Fig. 4 presents the milling time dependence of the *a* and *c* lattice parameters for the tetragonal copper ferrite structure ($I4_1/amd$), obtained after the heat treatment at 800 °C for 6 h. In the same figure are given for reference the values for the lattice parameters from JCPDS 34-0425 for $CuFe_2O_4$. The *a* lattice parameter value is close to the reference one, 5.844 Å (JCPDS 34-0425), for the samples milled for 8 and 12 h (5.845 and 5.848 Å) and it increases upon increasing the milling time up to 5.871 Å after 24 h of milling. The *c* lattice parameter is larger compared to the reference value, 8.630 Å (JCPDS 34-0425) and it decreases upon increasing milling time from 8.596 Å (4 h of milling) down to 8.514 Å (24 h of milling). These variations of the lattice parameter values are assumed to be influenced by the milling time that can lead to a change of the cations distribution and also by the samples contamination with iron. For this type of investigations, it is more suggestive if the crystal type is considered a tetragonally distorted spinel structure with non-standard face-centered space group $F4_1/ddm$, instead of $I4_1/amd$. The distortion is a Jahn–Teller origin and it is assigned to the alignment of the Cu^{2+} cations, occupying the octahedral spinel sublattice formed by the oxygen ions [17]. The conversion of the *a* lattice

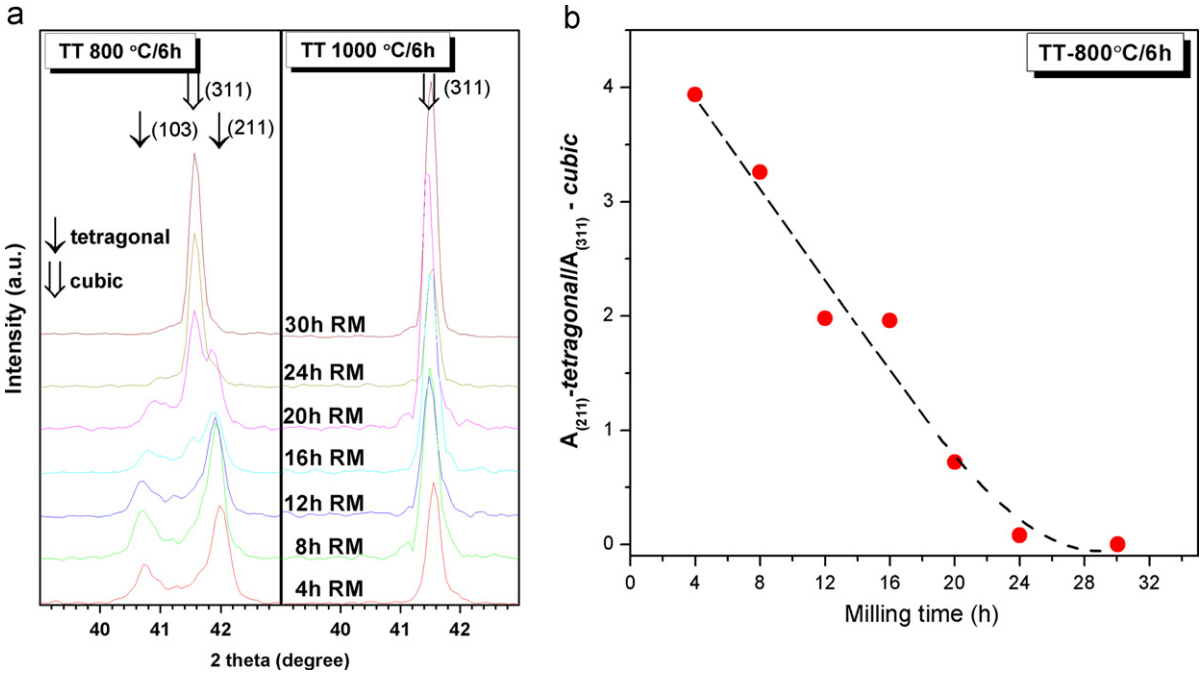

Fig. 3. (a) Details of the XRD patterns recorded for the samples milled for 4, 8, 12, 16, 20, 24 and 30 h and subsequently annealed at 800 °C and 1000 °C respectively for 6 h in air in 2θ interval where the most intense Bragg reflections of the tetragonal and cubic copper ferrite appear and (b) evolution of the area ratio between the most intense reflections of tetragonal structure (211) and cubic structure (311) versus milling time as derived for the samples heat treated at 800 °C for 6 h in air.

Table 1
Phases composition of the as-milled and the milled and subsequently annealed samples (6 h at 600, 800 and 1000 °C), according to XRD.

	4 h	8 h	12 h	16 h	20 h	24 h	30 h
After reactive milling	Fe_2O_3–CuO, c-$CuFe_2O_4$	Fe_2O_3–CuO, Cu_2O, c-$CuFe_2O_4$	Fe_2O_3–CuO, Cu_2O, c-$CuFe_2O_4$	Fe_2O_3–CuO, Cu_2O, c-$CuFe_2O_4$	Fe_2O_3–CuO, Cu_2O, Fe, c-$CuFe_2O_4$	Fe_2O_3–CuO, Cu_2O, Fe, Cu, c-$CuFe_2O_4$	Fe_2O_3–CuO, Cu_2O, Fe, Cu, c-$CuFe_2O_4$
600 °C/6 h	Fe_2O_3, CuO, t-$CuFe_2O_4$, c-$CuFe_2O_4$	Fe_2O_3, CuO, t-$CuFe_2O_4$, c-$CuFe_2O_4$	Fe_2O_3, CuO, t-$CuFe_2O_4$, c-$CuFe_2O_4$	Fe_2O_3, CuO, t-$CuFe_2O_4$, c-$CuFe_2O_4$	Fe_2O_3, CuO, t-$CuFe_2O_4$, c-$CuFe_2O_4$	Fe_2O_3, CuO, t-$CuFe_2O_4$, c-$CuFe_2O_4$	Fe_2O_3, CuO, c-$CuFe_2O_4$
800 °C/6 h	t-$CuFe_2O_4$, c-$CuFe_2O_4$	t-$CuFe_2O_4$, c-$CuFe_2O_4$	t-$CuFe_2O_4$, c-$CuFe_2O_4$	t-$CuFe_2O_4$, c-$CuFe_2O_4$	t-$CuFe_2O_4$, c-$CuFe_2O_4$	Fe_2O_3, t-$CuFe_2O_4$, c-$CuFe_2O_4$	Fe_2O_3, c-$CuFe_2O_4$
1000 °C/6 h	c-$CuFe_2O_4$	c-$CuFe_2O_4$	c-$CuFe_2O_4$	c-$CuFe_2O_4$	c-$CuFe_2O_4$	c-$CuFe_2O_4$	c-$CuFe_2O_4$

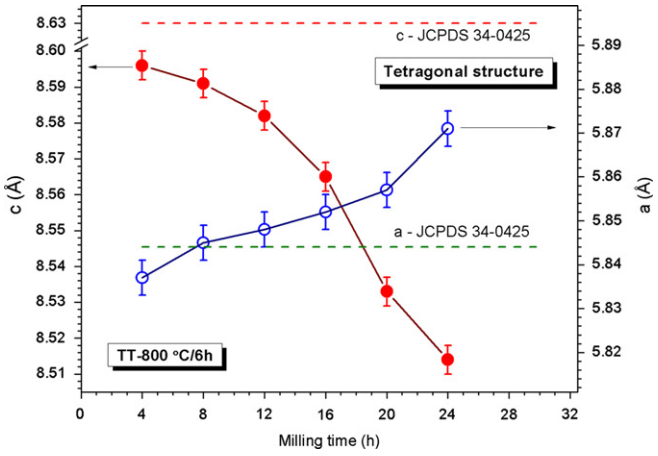

Fig. 4. Evolution of the *a* and *c* lattice parameters versus milling time for the tetragonal copper ferrite structure obtained after heat treatment at 800 °C for 6 h in air. For reference are given the *a* and *c* lattice parameters from JCPDS file no. 34-0425.

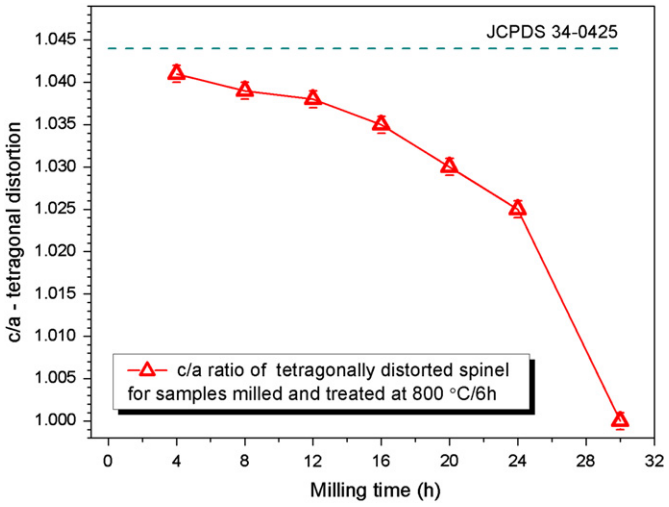

Fig. 5. Evolution of the *c*/*a* tetragonal distortion versus milling time.

parameter from the tetragonal structure ($I4_1/amd$) to cubic ($F4_1/ddm$) is given by $a_F = a_I\sqrt{2}$ (a_F—cubic $F4_1/ddm$ parameter and a_I—tetragonal $I4_1/amd$ parameter) [32]. The increase of the *a* lattice parameter and decrease of the *c* lattice parameter upon increasing milling time suggest the deformation of the tetragonally distorted spinel structure and transformation of this into a cubic one (Fd-3m). The *c*/*a* tetragonal distortion decreases upon increasing the milling time (Fig. 5) and practically the Jahn–Teller effect is diminished. This could happen if, after the milling process and subsequent heat treatment, the Cu^{2+} cations are distributed between the tetrahedral and octahedral sites. This indicates that the prolonged milling time is favourable to the Cu^{2+} cations arrangement in tetrahedral sites. The preference of the samples crystallisation in cubic spinel structure is assumed to be also influenced by the contamination with iron for longer milling time (20–30 h). The influence of the contamination with iron cannot be neglected for shorter milling time (4–16 h) even if the presence of iron was not detected by the XRD. The increase of the amount of iron in copper ferrite reduces the number of the copper cations per spinel cell and so, their possibility to occupy the tetragonal sites which cause the distortion.

The lattice parameter for the cubic structure that coexists with the tetragonal one, for the samples milled and heat treated at 800 °C for 6 h, is almost constant upon increasing the milling time. The calculated values of the lattice parameter are in 8.368–8.372 Å range and they are very close to the one from JCPDS file 77-0010 of pure copper ferrite. The evolution of the lattice parameter versus milling time for the cubic copper ferrite structure, obtained after the heat treatment in air at 800 °C and 1000 °C for 6 h, is presented in Fig. 6. For reference are given the values of the lattice parameter for the cubic $Cu_{1-x}Fe_{2-x}O_4$ from JCPDS 73-2315, 73-2316, 75-1517 and 77-0010. These parameters correspond to copper ferrites with different stoichiometry. The lattice parameter has different evolution for the samples heat treated at 1000 °C whereas, in all cases, the copper ferrite is crystallised in cubic spinel structure. Compared to the value of $CuFe_2O_4$ from JCPDS file 77-0010, 8.37 Å, the lattice parameter of these samples is larger, except the one calculated for the sample milled for 4 h, which is at almost the same value and the one of 30 h milled sample, which is very close. For further investigations regarding the influence of the iron provided by the contamination on the lattice parameter, the values of this were compared to the

ones of the copper ferrites with different content of supplementary iron, $Cu_{0.915}Fe_{2.085}O_4$, $Cu_{0.86}Fe_{2.14}O_4$ and $Cu_{0.75}Fe_{2.25}O_4$. By increasing the amount of iron in the copper ferrite, the lattice parameter becomes larger according to JCPDS files taken for comparison. For the samples milled for 8, 12, 16, 20 and 24 h and heat treated for 6 h at 1000 °C, the lattice parameter is closer to the one of the copper ferrite with small amount of supplementary iron, $Cu_{0.915}Fe_{2.085}O_4$. If the lattice parameter of the 30 h milled sample would have been closer to the one calculated for this ferrite, we could assume that this increase is mostly caused by the supplementary iron. So, it can be presumed that the evolution of the lattice parameter versus milling time is due to the different cations arrangement in cubic spinel rather than the presence of the supplementary iron cations.

Fig. 7 presents the magnetisation curves recorded at 300 K in a magnetic field up to 8 T for the samples obtained after 4, 8, 16, 24, 30 h of reactive milling and subsequent heat treatment at 800 °C for 6 h and, respectively, 1000 °C for 6 h. As can be remarked, there are two groups of curves, one for the samples heat treated at 800 °C and the other for the samples heat treated at 1000 °C. The magnetisation of the samples heat treated at 1000 °C is larger compared to the magnetisation of the samples heat treated at 800 °C. There are also some significant differences between the magnetisation of the samples heat treated at the same temperature depending on milling time. Therefore, the saturation magnetisation of each sample was calculated and its evolution versus milling time for both heat treatments is presented in Fig. 8. In the same figure are presented the saturation magnetisation values of the pure copper ferrite with inverse spinel structure and with partial inverse spinel structure (one of Cu^{2+} cation in tetrahedral site) and the normalised values of the saturation magnetisation at 100% copper ferrite for

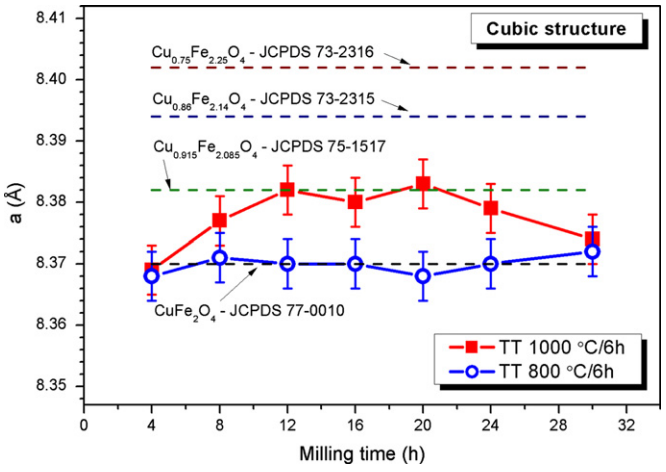

Fig. 6. Evolution of the lattice parameter, *a*, versus milling time for the cubic copper ferrite structure obtained after the heat treatment at 800 °C and 1000 °C for 6 h in air. For reference are given the lattice parameters from cubic $Cu_{1-x}Fe_{2-x}O_4$ compounds according to files JCPDS 73-2315, 73-2316, 75-1517 and 77-0010.

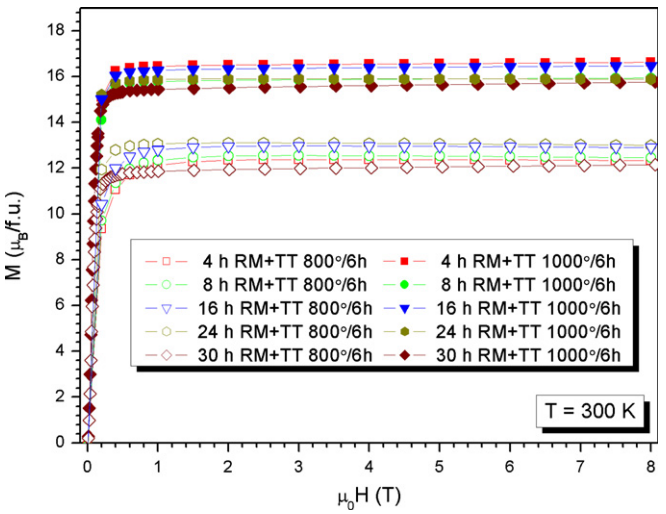

Fig. 7. Isothermal 300 K magnetisation curves recorded for the copper ferrite samples obtained after 4, 8, 16, 24, 30 h of reactive milling and subsequent heat treatment at 800 °C for 6 h and 1000 °C for 6 h in a maximum applied field of 8 T.

the samples heat treated at 800 °C. The saturation magnetisation of the samples heat treated at 800 °C increases from 12.4 μ_B/f.u. to 13.1 μ_B/f.u. upon increasing the milling time up to 24 h. This increase is followed by a decrease down to 11.9 μ_B/f.u. for the 30 h milled sample. The larger magnetisation of the samples milled for longer milling time is assumed to be provided by the increasing of the cubic copper ferrite amount, which probably leads to a different cations configuration in the spinel phase. On the other hand, in the 24 and 30 h milled samples, there are more iron cations in ferrite structure due to the powder contamination. This supplementary iron content can contribute to a larger magnetisation, but this contribution is somehow compensated by the presence of the α-Fe_2O_3, which is non-magnetic. That is why it can be assumed that the larger amount of the α-Fe_2O_3 in 30 h milled sample leads to a lower magnetisation compared to the samples milled for 24 h. Also, the normalised magnetisation of the 30 h milled sample is lower compared to the one of 24 h milled sample due to a different Cu/Fe cations ratio and different distribution of the cations in A and B sites. For all the samples heat treated at 800 °C, the magnetisation is larger in comparison to the one calculated for the inverse spinel structure (8 μ_B/f.u.), where the Cu^{2+} cations are exclusively located in the octahedral sites [2]. This suggests a different cations arrangement, a distribution of the copper and iron cations in both crystallographic sites. After the heat treatment at 1000 °C for all the milling times, the saturation magnetisation is much larger and close to the value of the partial inverse structure of $CuFe_2O_4$ with one Cu^{2+} in tetrahedral sites, 16 μ_B/f.u. [25]. For two of the samples, 4 and 16 h milled samples, the saturation magnetisation is larger, 16.4 and 16.3 μ_B/f.u., respectively. This suggests that more than one Cu^{2+} cation in the cubic spinel is located in the tetrahedral sites, taking into account that, for these samples, the presence of the

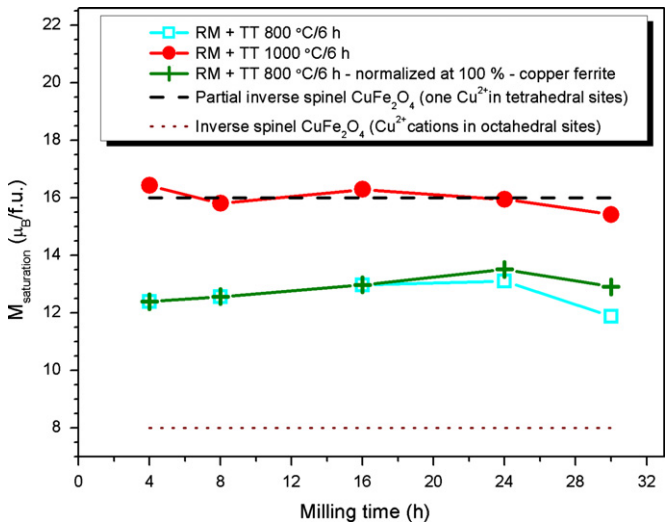

Fig. 8. Evolution of the saturation magnetisation of samples obtained after heat treatments at 800 °C and at 1000 °C for 6 h together with the evolution of saturation magnetisation normalised at 100% copper ferrite for the sample heat treated at 800 °C for 6 h as a function of milling time. For the reference are given the values of the magnetisation of the $CuFe_2O_4$ inverse spinel and partial inverse spinel (one Cu^{2+} cation is in the tetrahedral sites).

elemental Fe was not detected by XRD. However, the presence of the supplementary iron provided by the contamination and its influence on the magnetic properties cannot be completely excluded for these samples. Although, the supplementary iron content in the spinel does not automatically lead to an increase of the magnetisation as can be seen for the samples milled 24 and 30 h: 16 μ_B/f.u. and 15.4 μ_B/f.u. respectively. For these samples the presence of the supplementary iron was proved by XRD, but the saturation magnetisation is lower as compared to the ones of the samples milled for 4 and 16 h.

4. Conclusions

The reactive milling of the CuO and α-Fe_2O_3 stoichiometric mixture leads to the formation of various phases, depending on milling time. The milling process as a result of powder contamination supplies elemental iron, which changes the Cu/Fe ratio. The subsequent heat treatment at 600 °C in air is not sufficient for obtaining a complete reaction in mechano-activated samples. The copper ferrite is obtained for almost all milling times after the heat treatment at 800 °C and for all milling times after the heat treatment at 1000 °C. The crystal structure type of copper ferrite is influenced by the milling time and by powder contamination with iron for the samples heat treated at 800 °C. The tetragonal distortion decreases by increasing the milling time. The tetragonal structure is favoured by shorter milling time whereas cubic structure is favoured by longer milling time for this heat treatment. The milling time seems to have no influence on the copper ferrite crystallisation type in the samples annealed at 1000 °C, since for all milling times a cubic structure was obtained. The Cu^{2+} cations are distributed between tetrahedral and octahedral sites for both tetragonal and cubic structures. The copper ferrites with cubic structure obtained after heat treatment at 1000 °C present a larger magnetisation compared to the ones obtained after heat treatment at 800 °C, which are crystallised in both tetragonal and cubic structures. The values of magnetisation for cubic copper ferrites are close to the one calculated for the copper ferrite with partial inverse structure (one Cu^{2+} cations in tetrahedral sites).

Acknowledgement

This work was supported by CNCSIS–UEFISCSU, Project number PNII–IDEI code 1519/2008.

References

[1] A. Goldman, Modern Ferrite Technology, Second edition, Springer, Pittsburgh, 2006.
[2] B.D. Cullity, C.D. Graham, Introduction to Magnetic Materials, 2nd ed., IEEE Press & Wiley, New Jersey, 2009.
[3] M.A. Willard, Y. Nakamura, D.E. Laughlin, M.E. McHenry, Magnetic properties of ordered and disordered spinel-phase ferrimagnets, Journal of the American Ceramic Society 82 (12) (1999) 3342–3346.
[4] D.S. Mathew, R.S. Juang, An overview of the structure and magnetism of spinel ferrite nanoparticles and their synthesis in microemulsions, Chemical Engineering Journal 129 (2007) 51–65.
[5] E. Manova, T. Tsoncheva, D. Paneva, M. Popova, N. Velinov, B. Kunev, K. Tenchev, I. Mitov, Nanosized copper ferrite materials: mechanochemical synthesis and characterization, Journal of Solid State Chemistry 184 (2011) 1153–1158.
[6] K.E. Sickafus, J.M. Wills, Structure of spinel, Journal of the American Ceramic Society 82 (12) (1999) 3279–3292.
[7] E.J.W. Verwey, E.L. Heilmann, Cation arrangement in spinels, Journal of Chemical Physics 15 (4) (1947) 174–180.
[8] M. Gaudon, N. Pailhe, A. Wattiaux, A. Demourgues, Structural defects in AFe_2O_4 (A=Zn, Mg) spinels, Materials Research Bulletin 44 (2009) 479–484.
[9] J.A. Gomes, M.H. Sousa, F.A. Tourinho, J. Mestnik-Filho, R. Itri, J. Depeyrot, Rietveld structure refinement of the cation distribution in ferrite fine particles studied by X-ray powder diffraction, Journal of Magnetism and Magnetic Materials 289 (2005) 184–187.
[10] M.J. Akhtar, M. Nadeem, S. Javaid, M. Atif, Cation distribution in nanocrystalline $ZnFe_2O_4$ investigated using X-ray absorption fine structure spectroscopy, Journal of Physics: Condensed Matter 21 (2009) 405303 9pp.
[11] M. Srivastava, S. Chaubey, A.K. Ojha, Investigation on size dependent structural and magnetic behavior of nickel ferrite nanoparticles prepared by sol–gel and hydrothermal methods, Materials Chemistry and Physics 118 (2009) 174–180.
[12] V. Šepelák, A. Feldhoff, P. Heitjans, F. Krumeich, D. Menzel, F.J. Litterst, I. Bergmann, K.D. Becker, Non-equilibrium cation distribution, canted spin arrangement, and enhanced magnetization in nanosized $MgFe_2O_4$ prepared by a one-step mechanochemical route, Chemistry of Materials 18 (2006) 3057–3067.
[13] T.F. Marinca, I. Chicinaş, O. Isnard, V. Pop, F. Popa, Synthesis, structural and magnetic characterization of nanocrystalline nickel ferrite-$NiFe_2O_4$ obtained by reactive milling, Journal of Alloys and Compounds 509 (2011) 7931–7936.
[14] S. Ayyappan, S.P. Raja, C. Venkateswaran, J. Philip, B. Raj, Room temperature ferromagnetism in vacuum annealed $ZnFe_2O_4$ nanoparticles, Applied Physics Letters 96 (2010) 143106 3pp.

[15] N.S. Gajbhiye, G. Balaji, S. Bhattacharyya, M. Ghafari, Mössbauer studies of nanosize $CuFe_2O_4$ particles, Hyperfine Interactions 156/157 (2004) 57–61.
[16] J. Darul, Thermal instability of the tetragonally distorted structure of copper–iron materials, Zeitschrift Fur Kristallographie 30 (2009) 335–340.
[17] I. Nedkov, R.E. Vandenberghe, T. Marinova, P. Thailhades, T. Merodiiska, I. Avramova, Magnetic structure and collective Jahn–Teller distortions in nanostructured particles of $CuFe_2O_4$, Applied Surface Science 253 (2006) 2589–2596.
[18] J.Z. Jiang, G.F. Goya, H.R. Rechenberg, Magnetic properties of nanostructured $CuFe_2O_4$, Journal of Physics: Condensed Matter 11 (1999) 4063–4078.
[19] S.J. Stewart, R.C. Mercader, R.E. Vandenberghe, G. Cernicchiaro, R.B. Scorzelli, Magnetic anomalies and canting effects in nanocrystalline spinel copper ferrites $Cu_xFe_{3-x}O_4$, Journal of Applied Physics 97 (2005) 054304.
[20] D. Prabhu, A. Narayanasamy, K. Shinoda, B. Jeyadeven, J.-M. Greneche, K. Chattopadhyay, Grain size effect on the phase transformation temperature of nanostructured $CuFe_2O_4$, Journal of Applied Physics 109 (2011) 013532 6pp.
[21] V. Berbenni, A. Marini, C. Milanese, G. Bruni, Solid state synthesis of $CuFe_2O_4$ from $Cu(OH)_2$ $CuCO_3$-$4FeC_2O_4$ $2H_2O$ mixtures: mechanism of reaction and thermal characterization of $CuFe_2O_4$, Journal of Thermal Analysis and Calorimetry 99 (2010) 437–442.
[22] T.F. Marinca, I. Chicinaş, O. Isnard, Synthesis, structural and magnetic characterization of nanocrystalline $CuFe_2O_4$ as obtained by a combined method reactive milling, heat treatment and ball milling, Ceramics International 38 (2012) 1951–1957.
[23] S.J. Stewart, M.J. Tueros, G. Cernicchiaro, R.B. Scorzelli, Magnetic size growth in nanocrystalline copper ferrite, Solid State Communications 129 (2004) 347–351.
[24] R.A. Borzi, S.J. Stewart, G. Punte, R.C. Mercader, G. Cernicchiaro, F. Garcia, Glassy magnetic behavior in a nanostructured Cu–Fe–O system, Hyperfine Interactions 148/149 (2003) 109–116.
[25] G.F. Goya, H.R. Rechenberg, Reversibility of the synthesis–decomposition reaction in the ball-milled Cu–Fe–O system, Journal of Physics: Condensed Matter 10 (1998) 11829–11840.
[26] Y. Uehara, Polymorphic transformation in copper ferrite and maganite by grinding, Bulletin of the Chemical Society of Japan 45 (1972) 3209.
[27] T.F. Marinca, I. Chicinaş, O. Isnard, Influence of the heat treatment conditions on the formation of $CuFe_2O_4$ from mechanical milled precursors oxides, Journal of Thermal Analysis and Calorimetry 110 (2012) 301–307.
[28] J. Laugier, B. Bochu, CELREF V3, Developed at the Laboratoire des Materiaux et du Genie Physique, Ecole Nationale Superieure de Physique de Grenoble (INPG), 2003, 〈http://www.inpg.fr/LMGP〉.
[29] A. Barlet, J.C. Genna, P. Lethuillier, Insert for regulating temperatures between 2 and 1000 K in a liquid helium dewar: description and cryogenic analysis, Cryogenics 31 (1991) 801–805.
[30] T.F. Marinca, I. Chicinaş, O. Isnard, V. Pop, Structural and magnetic properties of nanocrystalline $ZnFe_2O_4$ powder synthesised by reactive ball milling, Optoelectronics and Advanced Materials Rapid Communications 5 (1) (2011) 39–43.
[31] T. Verdier, V. Nachbaur, M. Jean, Mechanosynthesis of zinc ferrite in hardened steel vials: influence of ZnO on the appearance of Fe(II), Journal of Solid State Chemistry 178 (2005) 3243–3250.
[32] P. Piszora, J. Darul, W. Nowicki, E. Wolska, Synchrotron X-ray powder diffraction studies on the phase transitions in $LiMn_2O_4$, Journal of Alloys and Compounds 362 (2004) 231–235.